Carbohydrate Polymer Technologies and Applications 2 (2021) 100140

Contents lists available at ScienceDirect

Carbohydrate Polymer Technologies and Applications

journal homepage: www.sciencedirect.com/journal/carbohydrate-polymer-technologies-and-applications

Modulating the controlled release of hydroxychloroquine mobilized on pectin films through film-forming pH and incorporation of nanocellulose

Giovana C. Zambuzi [a], Camilla H.M. Camargos [b], Maíra P. Ferreira [c], Camila A. Rezende [b], Osvaldo de Freitas [c], Kelly R. Francisco [a,*]

[a] Department of Natural Science, Mathematics and Education, Federal University of São Carlos – UFSCar, Araras, SP 13604-900, Brazil
[b] Department of Physical Chemistry, Institute of Chemistry, University of Campinas, Campinas, SP 13083-970, Brazil
[c] Department of Pharmaceutical Sciences, School of Pharmaceuticals Sciences of Ribeirao Preto, University of Sao Paulo, Ribeirao Preto, SP 14040-903, Brazil

ARTICLE INFO

Keywords:
Pectin
pH
Hydroxychloroquine
Nanocellulose
Drug release

ABSTRACT

Materials from renewable resources like pectin and nanocelluloses are useful for the controlled release of drugs such as hydroxychloroquine (HCQ), whose potential for treating tumor cells was recently verified. In this study, pectin films with HCQ were produced by casting at different pH values (4, 7, and 10). Additionally, pectin/HCQ membranes formed at pH 4 were incorporated with cellulose nanocrystals (CNC) and nanofibrils (CNF). Films are mainly amorphous with good compatibility between HCQ and pectin matrix. Release tests showed that films containing CNC and formed at pH 4 released the drug more slowly in phosphate buffer medium compared to other membranes. Additionally, film formed at pH 4 presented slower HCQ release at acid medium. The pectin platform proved to be an easy way to deliver HCQ with different kinetic rates by changing the pH and incorporating nanocellulose particles into the pectin film-forming solutions.

1. Introduction

The development of targeted drug delivery systems is greatly relevant for pharmaceutical applications, since it allows to overcome the limitations present in most common systems of therapeutic molecule delivery. Such drawbacks are associated with the occurrence of collateral effects (Hua, Marks, Schneider & Keely, 2015; Pastore, Kalia, Horstmann & Roberts, 2015). Biopolymers such as pectin and cellulose have been extensively researched to be used as platforms for the modified release of several drugs, mainly due to their promising characteristics such as biodegradability, biocompatibility, and non-toxicity. These materials also allow to control the drug release profile and extend its permanence in the organism (Auriemma et al., 2020; Hoare & Kohane, 2008; Oliveira et al., 2021; Ponrasu, Chen, Chou, Wu & Cheng, 2021). The use of biopolymer matrices as a drug delivery system for treating cancer cells, for example, has proven to favor the permeation of the drug into these cells and to promote its accumulation in tumors (Chevalier et al., 2017; Li et al., 2018; Sleightholm, Yang, Yu, Xie & Oupický, 2017; Wei, Senanayake, Warren & Vinogradov, 2013).

Likewise, polysaccharides have gained prominence as suitable materials for new processes and formulations to develop improved drug delivery systems (Del Gaudio et al., 2013; García-González, Jin, Gerth, Alvarez-Lorenzo & Smirnova, 2015; Sosnik, 2014). Besides its renewable origin and biocompatibility, pectin is suitable for human consumption, unexpensive, widely available, and exhibits amenability for surface chemistry functionalization (Meng et al., 2020; Mohamed, Alqahtani, Ahmad, Krishnaraju & Kalpana, 2021; Wang et al., 2016a). Found in the cell wall of various fruits and vegetables, especially citrus fruits, this carbohydrate polymer is classified as a heterogeneous acidic polysaccharide composed of D-galacturonic acid units linked by α-[1→4] glycosidic bonds, with partially esterified carboxylic groups (high methoxyl pectin or low methoxyl pectin) and high molecular weight (Cacicedo et al., 2018; Nasrollahzadeh, Sajjadi, Iravani & Varma, 2021; Sriamornsak, 2003). Its properties are usually explored in the food industry, where pectin is used as a natural gel and dairy stabilizer, and in pharmaceutical technologies for controlled release of formulations (Minzanova et al., 2018; Mironov, Shulepov, Ponomarev & Bakulev, 2013). The use of pectin in colon-targeted drug delivery system is an interesting application of this natural polymer. The system remains stable when passing through the intestinal tract, but it is digested by specific enzymes in the colon, where the drugs are then released (Kodoth, Ghate, Lewis, Prakash & Badalamoole, 2019; Moslemi, 2021;

* Corresponding author.
E-mail address: kfrancisco@ufscar.br (K.R. Francisco).

https://doi.org/10.1016/j.carpta.2021.100140
Received 24 June 2021; Received in revised form 9 August 2021; Accepted 19 August 2021
Available online 22 August 2021

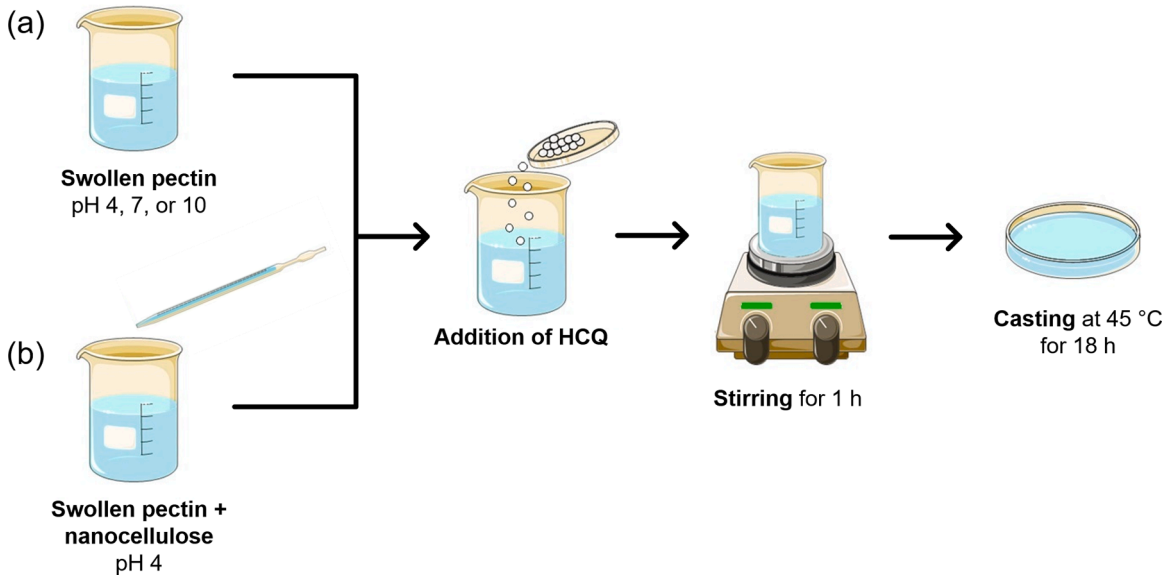

Fig. 1. Scheme showing the preparation of pectin films: (a) with hydroxychloroquine and (b) with hydroxychloroquine and nanocelluloses.

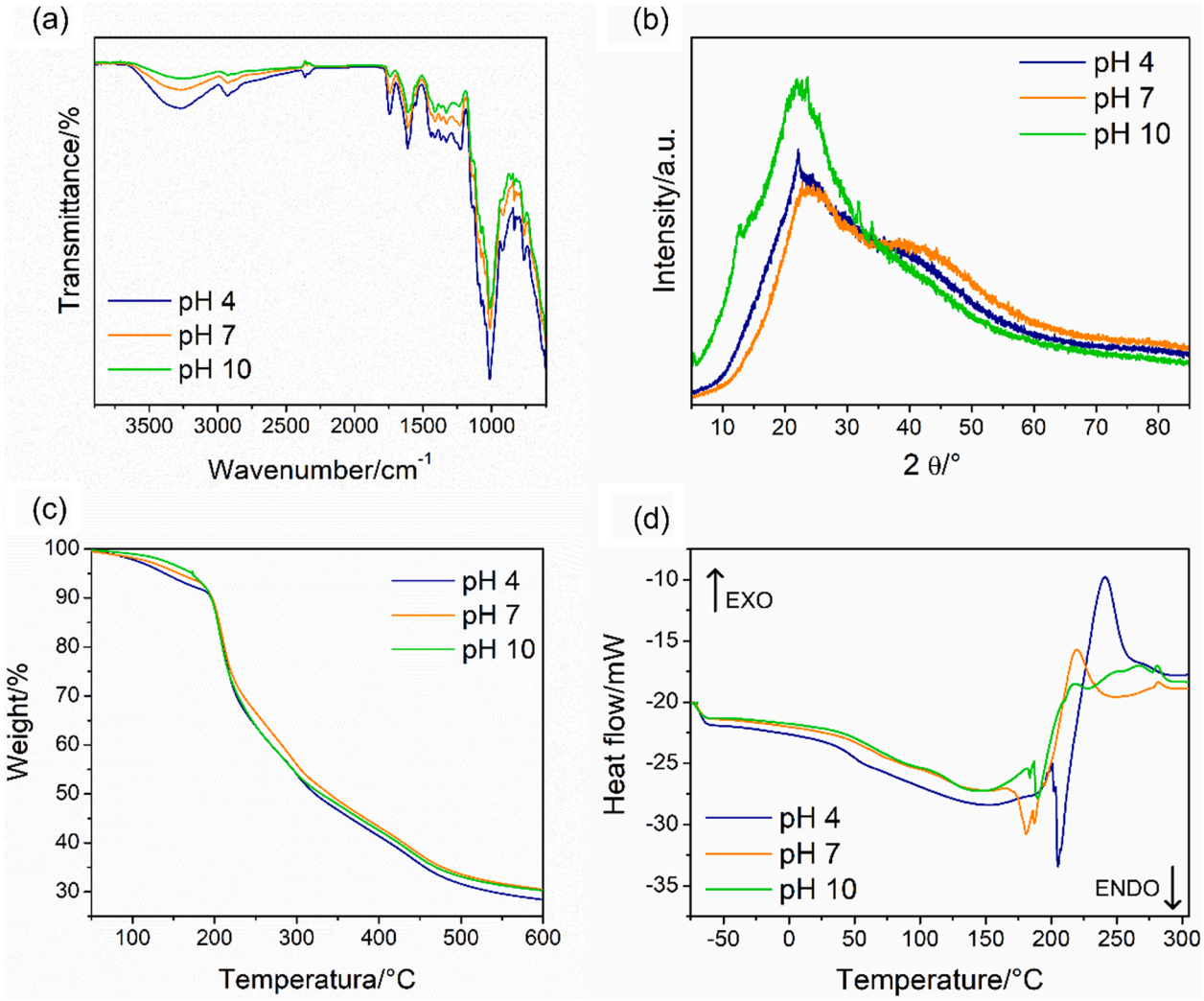

Fig. 2. (a) FTIR spectra, (b) x-ray diffractograms, (c) TGA, and (d) DSC curves of pectin films containing hydroxychloroquine formed by solutions at pH 4 (blue), pH 7 (orange), and pH 10 (green). (For interpretation of the references to color in this figure legend, the reader is referred to the web version of this article.)

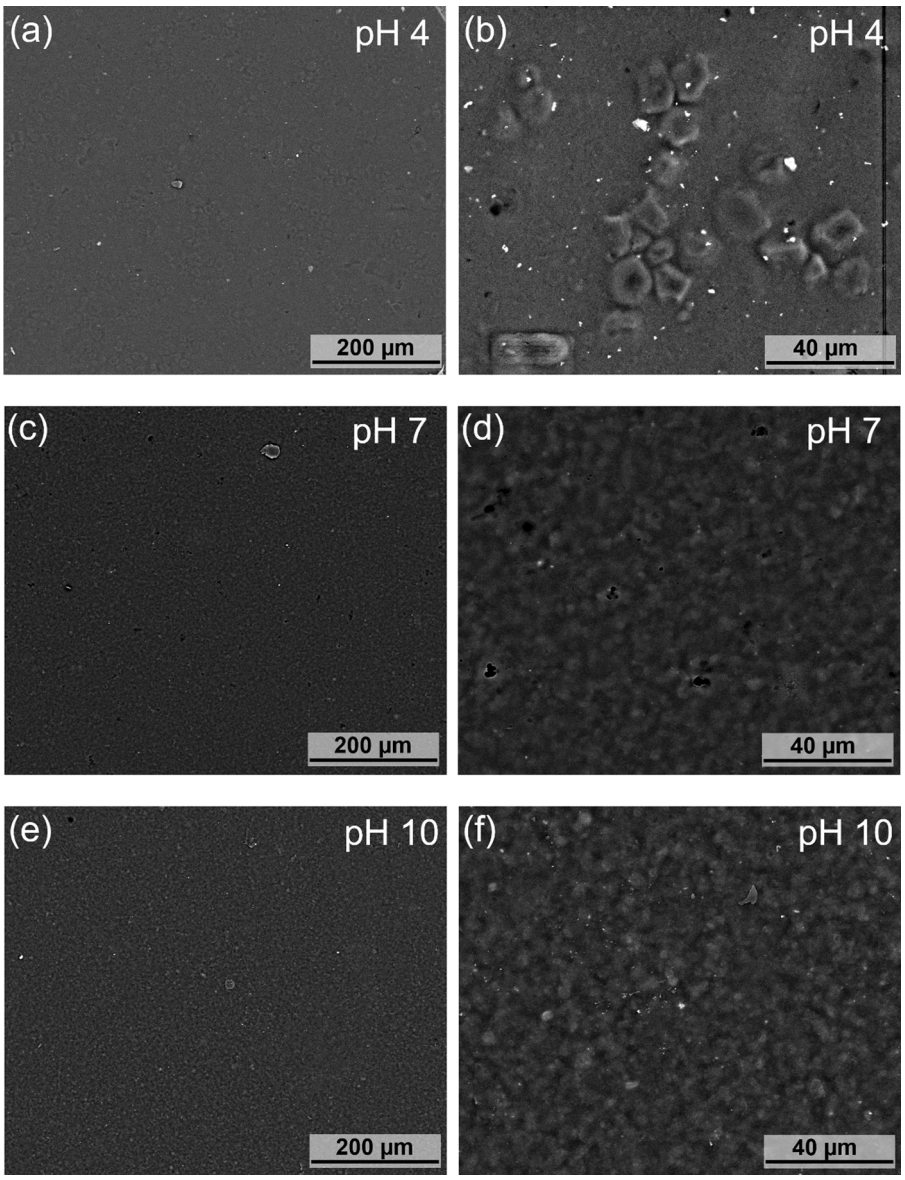

Fig. 3. SEM images of the surface of pectin films containing hydroxychloroquine formed by solutions at pH (a, b) 4, (c, d) 7, and (e, f) 10. Scale bars: (a, c, e) 200 μm and (b, d, f) 40 μm.

Vityazev et al., 2017). Some studies have also demonstrated the therapeutical use of pectin for gastric diseases, such as ulcer and intestine inflammations (Niu et al., 2021; Yan et al., 2011).

Hydroxychloroquine sulfate (HCQ) is recognized as being a less toxic derivative of chloroquine, which was initially developed for treating malaria in the 1940s. Currently, HCQ is used to treat lupus erythematosus, rheumatoid arthritis, skin diseases, with research indicating its ability to treat HIV (Bendas, Abdullah, El-Komy & Kassem, 2013; Chen et al., 2018; Richard et al., 2020). Recent studies have shown the ability of hydroxychloroquine to act as an adjunct drug for treating various types of cancers such as melanoma, breast, pancreas, and colon cancer by inhibiting cellular autophagy (Feng et al., 2019; Karasic et al., 2019; J. Liu et al., 2018a; Wang et al., 2016b ,2018; Yin et al., 2018). For these purposes, many studies mention formulations and different processes to produce HCQ delivery platforms, such as hard polymeric capsules, niosomes, pH-sensitive liposomes, chemically bonded hydroxyethyl starch/HCQ, polymer/nanoparticles/ ovalbumin nanovaccine, polyethylene glycol-functionalized gold nanoparticles, hollow mesoporous titanium dioxide nanoparticles, and pectin grafted onto Fe_3O_4 nanoparticles (Bendas et al., 2013; Feng et al., 2019; Liu et al., 2018a; Moraes et al., 2020; Perche et al., 2016; Sadr, Heydarinasab, Panahi & Javan, 2021; Sleightholm et al., 2017; Wang et al., 2016b,2018; Yin et al., 2018).

Thus, combining the properties of both pectin and HCQ is a promising approach to easily develop drug delivery platforms to treat colon cancer. However, literature on the use of this biopolymer as a platform for HCQ release is still lacking (Sadr et al., 2021). Furthermore, incorporating nanocelluloses into pectin/HCQ films can potentially prolong the drug release. Cellulose nanofibrils (CNF) have already been reported as a suitable reinforcing agent in starch/pectin free-standing films used for colonic methotrexate release. The incorporation of this nanofiller enhanced mucoadhesive, barrier, mechanical, and release profile properties of resistant films (Meneguin et al., 2017). Although the contribution of cellulose nanocrystals (CNC) to the controlled release of active molecules has also been gathering interest in biomedical field (Sheikhi et al., 2019), CNC-containing pectin delivery systems were not addressed so far.

Both CNF and CNC have outstanding surface area-to-volume ratio and can control the drug release mechanism due to high loading, interaction, and binding capacity for therapeutic molecules (Hasan

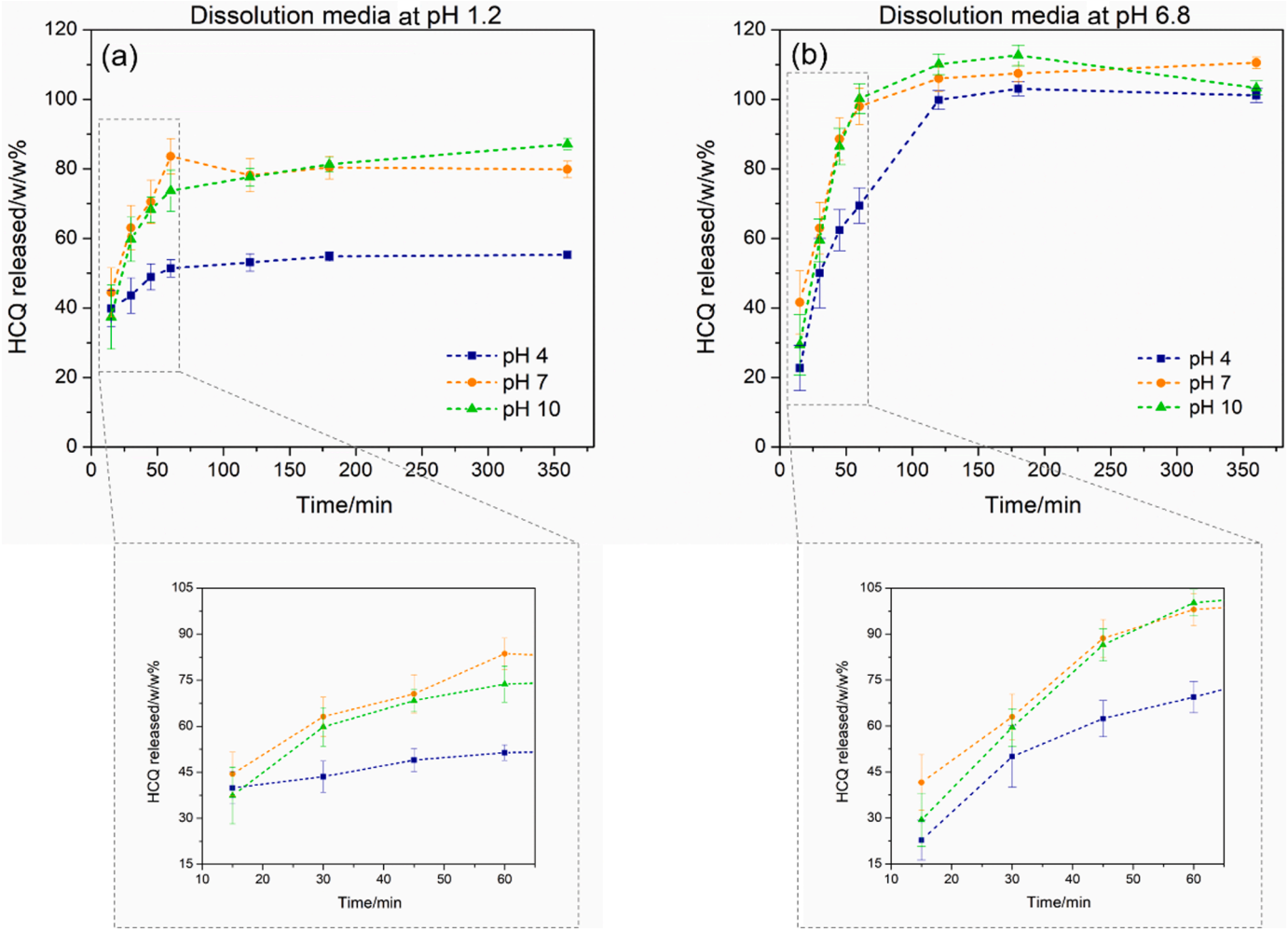

Fig. 4. HCQ release profile in dissolution media at: (a) pH 1.2 and (b) pH 6.8. The detailed amplified graphs highlight the HCQ release profiles in the first 60 min in the respective pH value. The HCQ molecules were mobilized on pectin films obtained from solutions at pH 4 (blue), 7 (orange), and 10 (green). (For interpretation of the references to color in this figure legend, the reader is referred to the web version of this article.)

et al., 2020). Having a high aspect ratio, CNF are thin (ca. 4 to 20 nm) and long (ca. 0.5 to 2 μm) cellulosic structures containing both amorphous and crystalline regions (Moon, Martini, Nairn, Simonsen & Youngblood, 2011). CNC, on the other hand, are usually obtained via acid hydrolysis of the amorphous areas of cellulose fibers and are much shorter structures (with lengths from 0.05 to 0.5 μm and similar diameter of CNF), composed mainly by crystalline domains (Mariño, Rezende & Tasic, 2018; Moon et al., 2011; Nascimento & Rezende, 2018). Nanocelluloses have been widely studied for several applications due to its interesting characteristics such as low density, high stiffness, high surface area, and biocompatibility (Du et al., 2019; Ghorbani, Roshangar & Soleimani Rad, 2020; Siqueira, Bras & Dufresne, 2010).

In this study, biopolymeric films containing pectin and hydroxychloroquine were prepared by casting at pH 4, pH 7, and pH 10. Pectin membranes containing both the drug and nanocellulose (CNC or CNF) were also produced at pH 4. Chemical composition, crystallinity, thermal behavior, and morphology of these biomaterials were studied by Fourier-transform infrared spectroscopy (FTIR), X-ray diffraction (XRD), thermogravimetric analysis (TGA), differential scanning calorimetry (DSC), and scanning electron microscopy (SEM). We evaluated the drug release profiles in acid and phosphate buffer medium to mimic the pH of the human digestive system and provide the release kinetics of the drug. The results showed that managing the physicochemical conditions of pectin film-forming solutions proved to be effective in modulating the drug release. Pectin films prepared at pH 4 and incorporated with CNC were able to retain the drug for longer in the polymeric matrix, thus providing a potential delivery platform for HCQ release in applications such as colon cancer treatment.

2. Experimental section

2.1. Materials

Milli-Q deionized water (resistivity: 18 MΩ cm) and aqueous solutions of citrus pectin (Genu® pectin type 105-RS from CP Kelco Brazil SA) were used throughout the process. Hydroxychloroquine sulfate (HCQ) was supplied by APSEN (Brazil); NaOH and HCl were purchased from Sigma-Aldrich. Cellulose nanocrystals were extracted from elephant grass leaves by sulfuric acid hydrolysis as previously described (Nascimento & Rezende, 2018). An adapted methodology was used to prepare cellulose nanofibrils by TEMPO (2,2,6,6-tetramethylpiperidine-1-oxyl radical)-mediated oxidation followed by sonication (Noronha et al., 2021; Saito, Kimura, Nishiyama & Isogai, 2007). All chemicals were used as received.

2.2. Preparation of pectin films

Solutions containing 3% (w/w) of citrus pectin were prepared by leaving pectin chains to solubilize on the bench at room temperature for 24 h, without stirring. Different pH values (4, 7, and 10) were achieved

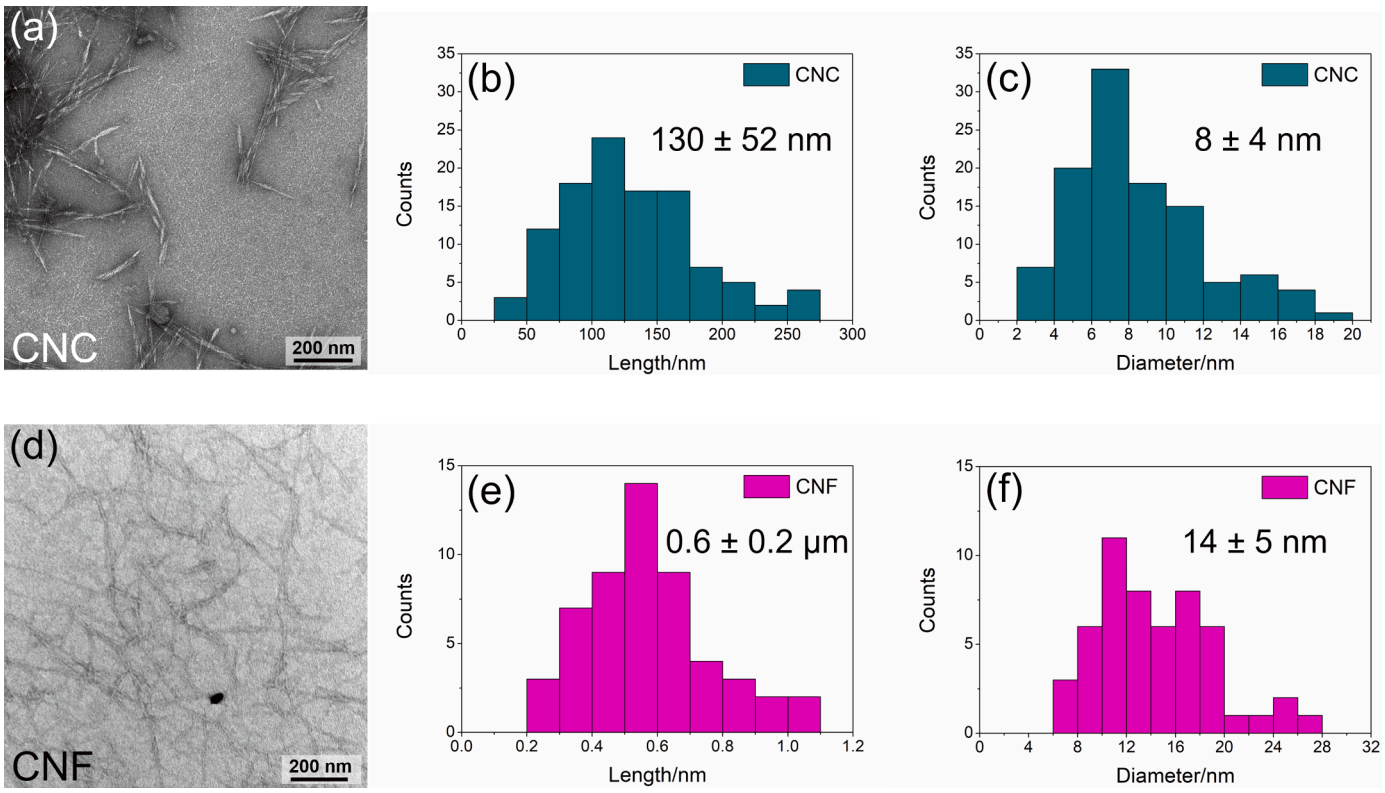

Fig. 5. TEM images of (a) cellulose nanocrystals and (d) cellulose nanofibrils. Scale bar: 200 nm. Size distribution histograms for (b, c) CNC and (e, f) CNF.

by adding small amounts of 0.1 mol/L NaOH or HCl to the pectin solutions. Hydroxychloroquine powder was added to the pectin solutions prepared at different pH conditions, followed by magnetic stirring for 1 h (Fig. 1(a)). Pectin films were formed by 75% (w/w) pectin and 25% (w/w) HCQ.

Films containing nanocellulose were prepared according to the same steps previously described, and adding dispersions of CNC or CNF to the 3% (w/w) pectin solutions at pH 4 prior to HCQ addition. Nanocellulose dispersions were added dropwise to the swollen pectin for 30 min under magnetic stirring, as to achieve a 2.5% (w/w) final concentration of nanoparticles in the dried films (Fig. 1(b)). Pectin/nanocellulose films consisted of 72.5% (w/w) pectin, 2.5% (w/w) nanocellulose and 25% (w/w) HCQ. After incorporating the hydroxychloroquine, all solutions and dispersions were placed in Petri dishes and dried in an oven at 45 °C for 18 h. The films were stored in desiccators for at least 48 h prior to analyses. The solubility of the films was determined by the loss of mass due to the contact with a buffer solution at pH 6.8, resulting in solubility ranging from 13 to 22 ± 2% in the first 120 min and 80 to 95% ± 1% in 24 h.

2.3. Methods

2.3.1. Fourier-transform infrared spectroscopy (FTIR)

FTIR spectra of pectin films with and without hydroxychloroquine were obtained by a Bruker FTIR Tensor II spectrometer, operating under attenuated total reflectance (ATR) or using a KBr insert holder. Spectra were obtained by accumulating 128 scans within the spectral range of 500 to 4000 cm^{-1} with a 4 cm^{-1} resolution.

2.3.2. X-ray diffraction (XRD)

Film crystallinity was assessed using a MiniFlex x-ray diffractometer (XRD - Rigaku), with CuK_{α} radiation (1.5418 Å), operating at 40 kV and 30 mA. Measurements were taken at room temperature, with an angular variation of 2θ between 2.0° and 70.0° and a scanning speed of 10.0°/min.

2.3.3. Thermogravimetric analysis (TGA) and differential scanning calorimetry (DSC)

The TGA of the pectin films was obtained using the PerkinElmer 4000 equipment under nitrogen atmosphere at 50 mL min^{-1}. Samples with initial weight varying from 4 to 10 mg were placed in ceramic sample holders and heated from 30 °C to 600 °C, with a 20 °C min^{-1} heating rate.

The DSC of the membranes (approximately 5 mg) was obtained by a PerkinElmer 4000 equipment under nitrogen atmosphere (flow rate of 50 mL/min), using a hermetically sealed aluminum holder. Samples were first cooled to –70 °C and kept in isotherm for 10 min, then heated to 230 °C at 10 °C/min.

2.3.4. Scanning electron microscopy (SEM)

Film morphology was analyzed in a Philips XL-30 FEG Bruker microscope, operating at 15 kV, using both secondary electron imaging (SEI) and backscattered electron imaging (BEI) modes. The films (1 cm x 1 cm) were fixed to the microscope sample holder and sputter coated with palladium-gold using a Bal-Tec Balzers SCD004 Sputter, operating at 15 mA for 60 s. We scanned ten representative micrographs of each sample.

2.3.5. Transmission electron microscopy (TEM)

The morphology of cellulose nanocrystals and nanofibrils was analyzed using a Carl Zeiss LIBRA 120 transmission electron microscope. CNC or CNF dispersions (5 µg/mL) were deposited on 400 mesh copper grids with carbon film, then dried at room temperature prior to analysis. CNC samples were stained with uranyl acetate 2% (v/v) before drying. Average size of CNC and CNF was estimated for a total of 150 and 110 nanoparticles, respectively, in TEM images using the ImageJ software (imagej.nih.gov).

2.3.6. Zeta potential measurements

Zeta potential of aqueous dispersions of CNC and CNF (50 µg/mL) was measured in triplicate using a Malvern Zetasizer® 300HS to

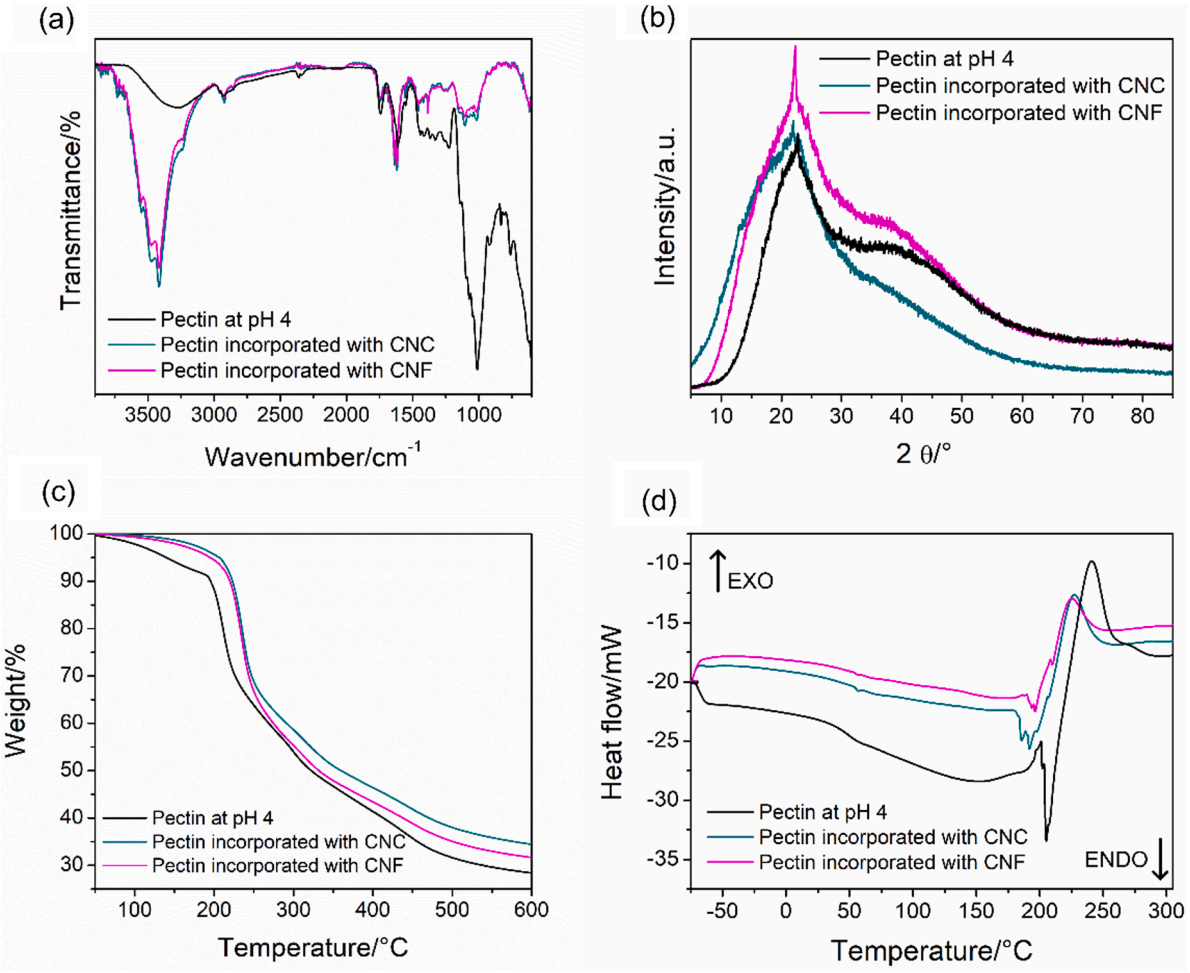

Fig. 6. (a) FTIR spectra, (b) XRD diffractograms, (c) TGA, and (d) DSC curves of pectin films formed at pH 4 containing HCQ and nanocellulose (CNC or CNF). Pectin film containing only HCQ (black) included for comparison. (For interpretation of the references to color in this figure legend, the reader is referred to the web version of this article.)

determine the surface charge density of the nanoparticles.

2.3.5. *Hydroxychloroquine modified release*

Hydroxychloroquine release from pectin films was evaluated in quintuplicate using the SOTAX® AT 7 equipment, according to the general USP method (United States Pharmacopeia 34th Ed Rockville (MD): US Pharmacop | Gaba Signaling, n.d.). Approximately 200 mg of film, which corresponds to ca. 50 mg of the drug, was added to the USP basket apparatus (apparatus 1) at 37 °C and 50 rpm. A total of 500 mL of sodium phosphate buffer (pH 6.8) or HCL solution (pH 1.2) was used as dissolution media. Aliquots of 1 mL were removed from the dissolution apparatus after 15, 30, 45, 60, 120, 180 and 360 min and filtered through a 0.22-μm membrane.

HCQ was quantified by UV–Vis spectroscopy using a Genesys 10S UV–Vis equipment at 343 nm and a calibration curve of the same wavelength (Mäntele & Deniz, 2017; Saini & Bansal, 2013).

3. Results and discussion

3.1. *Effect of pH on pectin film formation and HCQ release*

Pectin films with HCQ molecules are macroscopically homogeneous and become slightly opaque as the pH values of the film-forming solution decrease. Fig. 2 shows the chemical composition (FTIR), crystallinity (XRD) and thermal analysis (TGA and DSC) of the pectin films containing 250 mg/g of HCQ formed from solutions at different pH values (4, 7, and 10). FTIR, XRD, TGA, and DSC analysis of pectin and HCQ powders can be found in the Supplementary Material (Figs. S1, S2, S3, and S4, respectively).

FTIR spectra (Fig. 2(a)) of pectin films formed at different pH show similar profiles. The band at 3400 cm^{-1} was attributed to OH stretching of the pectin chains, HCQ, and hydration with water molecules, while the weak band around 2900 cm^{-1} was due to C–H stretching. Bands at approximately 1740, 1625, and 1440 cm^{-1} may be explained by the stretching of carboxylic groups (C=O ester), and the symmetric and asymmetric stretching of COO^{-} present in the macromolecule structure, respectively. The absorption band at around 1160–1010 cm^{-1} could be associated to the C–O–C (ether) and ring C–C bonds of galacturonic acid in pectin structure, and the strong band around 1010 cm^{-1} may be due to the stretching of the C–N–C and C–O groups of the hydroxychloroquine (Ansarifar, Mohebbi, Shahidi, Koocheki & Ramezanian, 2017; Engelsen & Nørgaard, 1996; Moraes et al., 2020). Our study associated the weak adsorption band at approximately 760 cm^{-1} to the C–Cl group in the HCQ molecule (Moraes et al., 2020). We observed no significant shifts in the characteristic absorption bands, indicating no significant change in the chemical composition of the produced films. Moreover, the FTIR spectra showed that pectin film formed at pH 4 presented band with a higher intensity absorption, suggesting a greater number of polar groups (O—H, COOH and C=O) on its surface than the other films, which indicated this film can create a higher number of hydrogen bonds among their polymeric chains and the drug.

XRD pattern of pectin powder (Fig. S2(a)) showed 2θ peaks at 8.3°,

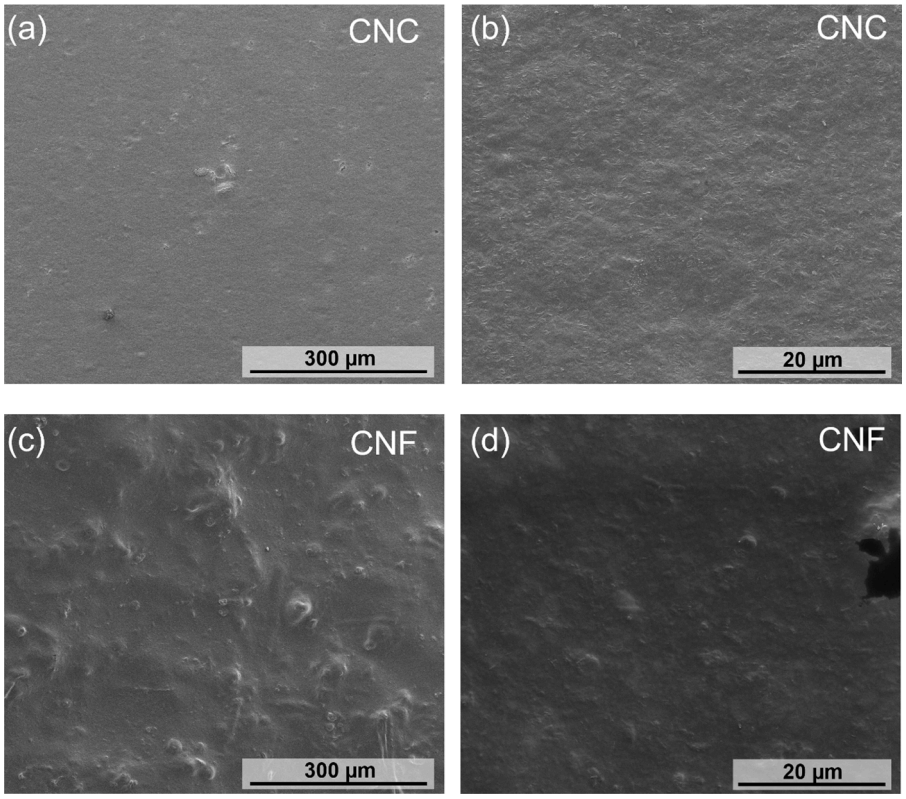

Fig. 7. SEM images of pectin/HCQ films prepared at pH 4 containing (a, b) CNC and (c, d) CNF. Scale bars: (a, c) 300 μm and (b, d) 20 μm.

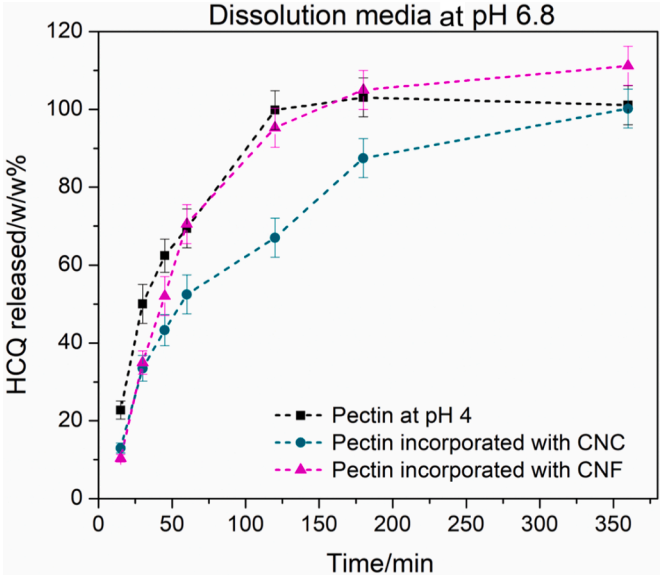

Fig. 8. Release profile of hydroxychloroquine in sodium phosphate buffer (pH 6.8) for pectin/HCQ films with cellulose nanocrystals (blue) and nanofibrils (magenta). Pectin/HCQ film formed at pH 4 (black) included for comparison. (For interpretation of the references to color in this figure legend, the reader is referred to the web version of this article.)

13.1°, 16.7°, 19.6°, 20.8°, 25.2°, 30.9°, and 38.2° corresponding to the backbone distance of the macromolecule, and indicating that the pristine pectin is a semicrystalline polymer (Mishra, Datt & Banthia, 2008). The XRD pattern of the HCQ powder (Fig. S2(b)) revealed various sharp and highly intense 2θ peaks at 12.4°, 16.8°, 19.8°, 21.6°, 23.7°, 26.5°, 28.7°, and 32.9°, confirming the HCQ crystallinity. XRD patterns of pectin films with HCQ (Fig. 2(b)), in turn, showed significant differences compared to the pure components, resulting in a considerable decrease in the amount and intensity of peaks, with a non-defined peak around 2θ = 23° and a broad shoulder at 2θ = 40° This result indicates that both the polymer and the drug had their crystallinities partially decreased during film formation. Such decline suggests the existence of good intermolecular interactions between pectin chains and HCQ molecules mainly due to electrostatic interactions and hydrogen bonds, and a consequent decrease in the intermolecular interactions between the pairs pectin-pectin chains and drug-drug molecules, a finding that was corroborated by the transparency and macroscopic homogeneity of the polymeric films, regardless of the pH of the film-forming solution (Li et al., 2014).

The TGA curves (Fig. 2(c)) indicated that the 5% weight loss temperature ($T_{5\%}$) was 138 °C, 154 °C, and 173 °C for pectin/HCQ films prepared at pH 4, 7, and 10, respectively. On the other hand, the decomposition temperature for a 10% weight loss ($T_{10\%}$) was around 195 °C for all the films, suggesting similar thermal stability for the samples. These temperatures are intermediate to the decomposition temperatures of pectin ($T_{5\%}$ of 134 °C and $T_{10\%}$ of 190 °C) and HCQ powder ($T_{5\%}$ of 203 °C and $T_{10\%}$ of 216 °C) (Fig. S3).

The DSC thermograms of all films showed a broad endothermic peak within the 80–145 °C range (Fig. 2(d)), resulting from the evaporation of water molecules retained in the biopolymer matrix (Di Donato et al., 2020; Slavutsky & Bertuzzi, 2019). A similar thermal event attributed to water release can be observed in the DSC curve of pure pectin as well (Fig. S4(a)). Pectin also presented an endothermic dip with minimum at 196 °C and an exothermic peak at 237 °C, explained by the melting and degradation of the biopolymer, respectively (Fig. S4(a)). HCQ molecules showed a melting point at 249 °C and an endothermic peak at 276 °C (Fig. S3(b)). The DSC curve of the film formed at pH 4 presented a small endothermic shoulder at 202 °C and an endothermic peak at 205 °C (Fig. 2(c)), due to the melting of the polymer and the drug crystals, respectively. The decreased drug melting point indicates that the

Table 1
Fitted parameters using Zero order, First order, Higuchi and Korsmeyer-Peppas models for the HCQ release kinetics.

HCQ release at pH 1.2				
Model	Parameters	Film formed at pH 4	Film formed at pH 7	Film formed at pH 10
Zero order	R^2	0.74	0.54	0.74
First order	k_1	7.04×10^{-4}	0.0019	0.0037
	R^2	0.76	0.54	0.88
Higuchi	k_H	0.9218	1.7077	2.5835
	R^2	0.84	0.66	0.83
Korsmeyer-Peppas	n	0.1055	0.1621	0.232
	k_{K-P}	3.4469	3.5575	3.2174
	R^2	**0.93**	**0.80**	**0.89**
HCQ release at pH 6.8				
Model	Parameters	Film formed at pH 4	Film formed at pH 7	Film formed at pH 10
Zero order	R^2	0.76	0.68	0.58
First order	k_1	0.059	0.075	0.055
	R^2	**0.96**	**0.97**	**0.98**
Higuchi	k_H	4.923	3.846	4.1038
	R^2	0.86	0.79	0.71
Korsmeyer-Peppas	n	0.4512	0.2910	0.3681
	k_{K-P}	2.2552	3.1848	2.7998
	R^2	0.91	0.88	0.82
HCQ release at pH 6.8 (films with nanocellulose)				
Model	Parameters	Pectin film formed at pH 4 with CNC	Pectin film formed at pH 4 with CNF	
Zero order	R^2	0.90	0.82	
First order	k_1	0.0108	0.0286	
	R^2	**0.98**	**0.99**	
Higuchi	k_H	5.6201	6.5767	
	R^2	0.97	0.91	
Korsmeyer-Peppas	n	0.6002	0.6975	
	k_{K-P}	1.3078	1.0264	
	R^2	0.95	0.90	

intermolecular interactions between HCQ molecules became weaker in the film, resulting in a good dispersion of the drug in the polymeric matrix, as confirmed by XRD analysis (Li et al., 2014; Saini & Bansal, 2013). For pectin membranes formed at pH 7 and 10, two melting peaks are visible due to the melting point of the polymer and HCQ. For the films formed at pH 7, the 180 °C and 187 °C melting points referred to pectin and HCQ, respectively. Films formed at pH 10 showed melting points at 187 °C and 190 °C. Exothermic events, in turn, occurred at 241 °C, at 220 °C, and at 220 °C–280 °C for films formed at pH 4, 7, and 10, respectively. These events could result from the sample degradation processes (Nawrocka, Szymańska-Chargot, Miś, Wilczewska & Markiewicz, 2017; Zhang et al., 2020), indicating that an increment in the pH values of the film-forming solution led to a decrease in the intermolecular interactions between the biopolymer and the drug, as the melting point and the degradation occurred at lower temperatures. The exothermic peak concerning the degradation of the films prepared at higher pH values encompassed a broad temperature range. Such behavior was likely due to the higher surface charge of the pectin chains at high pH condition, as well as to the chemical reactions occurring during the drying process, resulting in pectin chains with different molar mass (Fracasso et al., 2018; Nascimento et al., 2019).

The micrographs in Fig. 3 show that pectin films with HCQ presented heterogeneous surfaces, with HCQ crystals dispersed on the polymeric matrix. Despite the heterogeneities observed due to the presence of HCQ crystals at lower pH, the overall aspect of the pectin film formed at pH 4 (Fig. 3(b)), even coating HCQ crystals, was more compact than that of the films formed at pH 7 and 10. This profile could result from the dependence of pectin chain conformation on the pH solution, which produced a less compact and rougher film at higher pH (Fig. S5). Therefore, pectin surface charge influences the film morphology, as reported by Nascimento et al. (2019).

Differences in the film surfaces due to the self-assembly of pectin chains and HCQ at different pH values could influence the mechanism and release of the drug in aqueous medium. Fig. 4 shows the HCQ releases in dissolution media of pH 1.2 and 6.8.

The results showed that films formed from pectin solutions at lower pH presented slower HCQ release compared to films formed at pH 7 and 10. This result suggests that good intermolecular interactions between polymeric chains and the drug in the pectin films, combined with a more compact surface, played an important role in HCQ release. In fact, Silva Favacho et al., 2020) showed that mucoadhesive orodispersible tablets of prilocaine and lidocaine had higher release rates in polymeric matrices with a higher number of porous structures due to an increase in the drug dissolution and permeation, and that the capillarity effect on these structures increased the interaction between the drugs and the aqueous medium. Thus, the surface charge of pectin solutions can influence the conformation of polymeric chains in the solid phase, and, consequently, the morphology and roughness of the film surfaces. The rougher the film surface, the more prone the biopolymer chains are to interact with the water molecules in the medium, either by capillarity phenomena or as a result of the high surface area, leading to the solubilization of the film and increased drug release.

Pectin films formed at pH 4 showed a significantly slower release of HCQ molecules in lower pH dissolution medium, with the cumulative drug release after 360 min in the aqueous medium at pH 1.2 and pH 6.8 reaching approximately 55% and 100%, respectively. As pectin has a pH-dependent solubility, the polymeric chains show resistance to solubilization in pH lower than 5.0, while at higher pH the macromolecule is readily dissolved (Khotimchenko, 2020; Wang et al., 2020; Wong, Colombo & Sonvico, 2011). Consequently, the drug release in the digestive system decreased. This result corroborates other studies where HCQ molecules were released by platforms obtained in a more complex way, such as nanoparticles and niosomes materials (Bendas et al., 2013; Feng et al., 2019; Sadr et al., 2021).

3.2. Morphology and colloidal stability of CNC and CNF

The cellulose nanocrystals and nanofibrils extracted from elephant grass leaves and later incorporated into the pectin films presented typical morphology. CNC had needle-like shape (Fig. 5(a)), were 130 ± 52 nm long (Fig. 5(b)) and 8 ± 4 nm wide (Fig. 5(c)), with an aspect ratio of 23 ± 9. CNF, in turn, presented a nanofibrillated network morphology (Fig. 5(d)), were 0.6 ± 0.2 μm long (Fig. 5(e)) and 14 ± 5 nm wide (Fig. 5(f)), with a higher aspect ratio of 53 ± 18.

In aqueous dispersion at pH 4, CNC and CNF presented zeta potentials of –41 ± 5 mV and –46 ± 4 mV, respectively. The very negative zeta potential values indicate that these nanoparticles were sufficiently stabilized by electrostatic repulsion in water (Evans & Wennerström, 1999; Noronha et al., 2021). When incorporated into pectin film-forming solutions at pH 4, the cellulose nanostructures would likely be uniformly dispersed.

3.3. Effect of nanocellulose on pectin film formation and HCQ release

As pectin film with HCQ formed at pH 4 proved to be a suitable material for drug-controlled release, its properties underwent a new evaluation after the addition of nanocellulose. Fig. 6 presents the FTIR spectra, XRD patterns, TGA and DSC curves of the pectin films containing CNC and CNF.

FTIR spectra of pectin films containing HCQ and nanocelluloses (Fig. 6(a)) showed a broad band around 3500 cm^{-1} that was attributed to the stretching of OH groups present in pectin, in HCQ, and in nanocelluloses (Engelsen & Nørgaard, 1996; Thomas et al., 2021). The relative intensity of this adsorption band was stronger in the composite membranes than in the film, as nanocellulose has several OH groups in its chemical structure (Heise et al., 2021). Besides pectin and HCQ

absorption bands, the spectra registered a band at 1640 cm^{-1} associated to adsorbed water and cellulose fingerprint absorption bands at around 1100 and 1020 cm^{-1}, attributed to C–O–C or C–O stretching (Pereira, Ornaghi Júnior, Coutinho, Duchemin & Cioffi, 2020).

The XRD results (Fig. 6(b)) indicate that pectin films with HCQ and nanocellulose are mainly amorphous, exhibiting a peak at approximately $2\theta = 22°$, which may be due to both the drug and cellulose (Jordan, Easson, Dien, Thompson & Condon, 2019; Pereira et al., 2020). These nanocellulose-containing membranes also presented good compatibility between film components, as shown by the macroscopic homogeneity and transparency of the materials.

TGA curves showed that the incorporation of CNC and CNF improved the thermal stability of the pectin film formed at pH 4 (Fig. 6(c)). Thermal decomposition ($T_{10\%}$) increased from 196 °C in the pectin film to 220 °C in the CNF-containing and 223 °C in CNC-containing pectin films. This improvement in thermal resistance could be attributed to strong interactions between pectin/HCQ matrix and the nanofillers (Meneguin et al., 2017).

Fig. 6(d) presents the DSC thermograms of the films containing HCQ and nanocellulose. Films with CNF of CNC showed two endothermic peaks regarding the melting point of the pectin and the drug, respectively: for CNC-containing films, the melting temperatures were 185.6 °C and 191.8 °C; while for the CNF-containing films the temperatures were 193.9 °C and 196.2 °C. In both cases, the degradation processes of pectin films occurred at around 225 °C. The main difference between the DSC results of pectin films with and without nanocellulose was the broad endothermic peak in the range of 80–145 °C, attributed to the evaporation of water molecules, which did not occur in the presence of CNC and CNF.

Fig. 7 shows the SEM micrographs of the pectin/HCQ films containing nanocellulose. While the pectin/HCQ membrane with CNC had a smoother and homogeneous surface, the pectin/HCQ film containing CNF presented a rougher and more heterogeneous surface, with agglomerated particles of different sizes and shapes. This result suggests that the individualized nanocrystals were homogeneously dispersed in the polymeric matrix, whereas the nanofibrils were only partially incorporated into it, remaining on the film surface and aggregating during the drying process, as reported by other studies (Liu, Zhong, Huang & Li, 2014; Silva et al., 2021). The network-like morphology formed after CNF drying (Fig. 5(d)) may also justify this observation. The self-assembly capacity of nanocelluloses can influence the drug release from pectin films, either via intermolecular interactions – mainly hydrogen bonds – or by acting as a physical barrier, decreasing material solubility. Fig. 8 shows the cumulative HCQ release profile of pectin films containing cellulose nanocrystals and nanofibrils in sodium phosphate buffer (pH 6.8).

HCQ molecules showed a slower release from the CNC-pectin film compared to the film with CNF. During the first 120 min, the drug release from the pectin films containing CNC and CNF were approximately 65% and 95%, respectively. Films with or without nanofibrils had the same cumulative release profile. This result indicates that the high specific surface area of CNC and its better dispersion in the matrix allowed for stronger intermolecular interactions with HCQ and pectin chains (both hydrogen bonds and van der Waals), reducing the solubilization of the film in the medium. While CNC loads can increase the solubility of poorly water-soluble drugs, the strong interaction with this nanofiller promotes the release of water-soluble drugs, such as HCQ, on a sustained fashion (Raghav, Sharma & Kennedy, 2021). Consequently, the presence of CNC increased the retention time of the drug in the polymeric matrix compared to the other films evaluated. HCQ release, in turn, showed a higher rate in films containing CNF due to the nanoparticle agglomeration and consequent surface heterogeneity. Thus, when cellulose nanofibril agglomerates detach from the polymeric matrix, a large amount of the drug interacting with CNF may be released. Similar results were found using polymers and nanocellulose particles as a vehicle to deliver different drugs, for instance, gelatin criogels with nanocellulose prepared by cross-linking and used as carriers of 5-fluorouracil, films of dextran and nanocellulose prepared by layer-by-layer technique to encapsulate the anticancer drug curcumin, starch/pectin films with nanocellulose as platform to release methotrexate and others (Anirudhan, Binusreejayan & Christa, 2017; Laurén et al., 2018; Li et al., 2019; Liu et al., 2018b; Meneguin et al., 2017; Paulraj, Riazanova & Svagan, 2018; Anirudhan, Chithra, Shainy and Thomas, 2019).

To evaluate the HCQ release kinetics in pectin films, we considered four different mathematical models widely used for this purpose, namely, zero order (Eq. (1)), first order (Eq. (2)), Higuchi (Eq. (3)) and Korsmeyer-Peppas (Eq. (4)) (Costa & Sousa Lobo, 2001; Korsmeyer, Gurny, Doelker, Buri & Peppas, 1983; Peppas & Khare, 1993):

$$Q_t = k_0 t \quad (1)$$

$$Q_t = 1 - e^{k_1 t} \quad (2)$$

$$Q_t = k_H \sqrt{t} \quad (3)$$

$$Q_t = k_{K-P}\, t^n \quad (4)$$

where Q_t is the fractional drug release at time; k_0, k_1, k_H and $k_{K\text{-}P}$ are the release constants for each release kinetic model; n is the diffusion exponent. Table 1 presents the fitted parameters and the regression coefficient (R^2) for each model of the HCQ release in pectin films.

According to the results above, the Korsmeyer-Peppas model presented a better fit for the release of HCQ from pectin films in acidic medium (pH 1.2), as indicated by the higher R^2 value. The diffusion exponent was $n < 0.5$ for all HCQ-pectin films, indicating that the drug release mechanism is driven by diffusion and obeys Fick's first law. The kinetic release of the drug from pectin membranes in phosphate buffer (pH 6.8) was adjusted with the best linearity by the first order model, where the drug release rate is a function of the drug content remaining in the films and the diffusion phenomenon is predominant.

4. Conclusion

This study showed that controlling pectin film-forming pH and adding nanocellulose particles was a simple way to modulate the interactions between polymeric chains and HCQ molecules, consequently modifying the drug release rate. We were able to control the HCQ release from pectin platforms by varying the pH of the dissolution aqueous media, since the drug release in acid medium is slower than in phosphate buffer. As such, pectin films prepared at pH 4 and containing cellulose nanocrystals could be the most efficient option for potential application in colon cancer treatment and for processes that require a slower action of the drug in the body.

Declaration of Competing Interest

The authors declare no conflict of interest.

Acknowledgements

We thank the financial support of the São Paulo Research Foundation (FAPESP, grants 2017/20006–4 and 2018/23769–1) and the Brazilian Council for Scientific and Technological Development (CNPq, grant 420031/2018–9). Authors G. C. Z and C. H. M. C. hold a fellowship from FAPESP (grant 2018/12146–3) and CNPq (grant 140558/2017–9), respectively. The authors thank the Laboratory of Structural Characterization (LCE/DEMa/UFSCar) for the general facilities, Dr. Douglas Soares da Silva and INCT-INOMAT for providing access to the TEM facility, and IQ-UNICAMP for providing infrastructure and access to DLS equipment. The authors thank Espaço da Escrita – Pró-Reitoria de Pesquisa – UNICAMP for the language services provided.

Supplementary materials

Supplementary material associated with this article can be found, in the online version, at doi:10.1016/j.carpta.2021.100140.

References

Anirudhan, T. S., Binusreejayan, & Christa, J. (2017). Multi-polysaccharide based stimuli responsive polymeric network for the: In vitro release of 5-fluorouracil and levamisole hydrochloride. *New Journal of Chemistry, 41*(20), 11979–11990. https://doi.org/10.1039/c7nj01745f.

Ansarifar, E., Mohebbi, M., Shahidi, F., Koocheki, A., & Ramezanian, N. (2017). Novel multilayer microcapsules based on soy protein isolate fibrils and high methoxyl pectin: Production, characterization and release modeling. *International Journal of Biological Macromolecules, 97*, 761–769. https://doi.org/10.1016/j.ijbiomac.2017.01.056.

Auriemma, G., Cerciello, A., Aquino, R. P., Del Gaudio, P., Fusco, B. M., & Russo, P. (2020). Pectin and zinc alginate: The right inner/outer polymer combination for core-shell drug delivery systems. *Pharmaceutics, 12*(2), 87. https://doi.org/10.3390/pharmaceutics12020087.

Bendas, E. R., Abdullah, H., El-Komy, M. H. M., & Kassem, M. A. A. (2013). Hydroxychloroquine niosomes: A new trend in topical management of oral lichen planus. *International Journal of Pharmaceutics, 458*(2), 287–295. https://doi.org/10.1016/j.ijpharm.2013.10.042.

Cacicedo, M. L., Islan, G. A., Drachemberg, M. F., Alvarez, V. A., Bartel, L. C., Bolzán, A. D., et al. (2018). Hybrid bacterial cellulose-pectin films for delivery of bioactive molecules. *New Journal of Chemistry, 42*(9), 7457–7467. https://doi.org/10.1039/c7nj03973e.

Chen, Y., Traore, Y. L., Yang, S., Lajoie, J., Fowke, K. R., Rickey, D. W., et al. (2018). Implant delivering hydroxychloroquine attenuates vaginal T lymphocyte activation and inflammation. *Journal of Controlled Release, 277*, 102–113. https://doi.org/10.1016/j.jconrel.2018.03.010.

Chevalier, M. T., Rescignano, N., Martin-Saldaña, S., González-Gómez, Á., Kenny, J. M., San Román, J., et al. (2017). Non-covalently coated biopolymeric nanoparticles for improved tamoxifen delivery. *European Polymer Journal, 95*, 348–357. https://doi.org/10.1016/j.eurpolymj.2017.08.031.

Costa, P., & Sousa Lobo, J. M. (2001). Modeling and comparison of dissolution profiles. In *European journal of pharmaceutical sciences, 13* pp. 123–133). Elsevier. https://doi.org/10.1016/S0928-0987(01)00095-1.

Del Gaudio, P., Auriemma, G., Mencherini, T., Porta, G. Della, Reverchon, E., & Aquino, R. P. (2013). Design of alginate-based aerogel for nonsteroidal anti-inflammatory drugs controlled delivery systems using prilling and supercritical-assisted drying. *Journal of Pharmaceutical Sciences, 102*(1), 185–194. https://doi.org/10.1002/jps.23361.

Di Donato, P., Taurisano, V., Poli, A., Gomez d'Ayala, G., Nicolaus, B., Malinconinco, M., et al. (2020). Vegetable wastes derived polysaccharides as natural eco-friendly plasticizers of sodium alginate. *Carbohydrate Polymers, 229*, Article 115427. https://doi.org/10.1016/j.carbpol.2019.115427.

Du, H., Liu, W., Zhang, M., Si, C., Zhang, X., & Li, B. (2019). Cellulose nanocrystals and cellulose nanofibrils based hydrogels for biomedical applications. In *Carbohydrate polymers, 209* pp. 130–144). Elsevier Ltd. https://doi.org/10.1016/j.carbpol.2019.01.020.

Engelsen, S. B., & Nørgaard, L. (1996). Comparative vibrational spectroscopy for determination of quality parameters in amidated pectins as evaluated by chemometrics. *Carbohydrate Polymers, 30*(1), 9–24. https://doi.org/10.1016/S0144-8617(96)00068-9.

Evans, D. F., & Wennerström, H. (1999). *The colloidal domains. Where physics, chemistry, biology, and technology meet* (2nd ed). Wiley-VCH.

Feng, Q., Yang, X., Hao, Y., Wang, N., Feng, X., Hou, L., et al. (2019). Cancer cell membrane-biomimetic nanoplatform for enhanced sonodynamic therapy on breast cancer via autophagy regulation strategy. *ACS Applied Materials and Interfaces, 11*(36), 32729–32738. https://doi.org/10.1021/acsami.9b10948.

Fracasso, A. F., Perussello, C. A., Carpiné, D., Petkowicz, C. L., de, O., & Haminiuk, C. W. I. (2018). Chemical modification of citrus pectin: Structural, physical and rheologial implications. *International Journal of Biological Macromolecules, 109*, 784–792. https://doi.org/10.1016/j.ijbiomac.2017.11.060.

García-González, C. A., Jin, M., Gerth, J., Alvarez-Lorenzo, C., & Smirnova, I. (2015). Polysaccharide-based aerogel microspheres for oral drug delivery. *Carbohydrate Polymers, 117*, 797–806. https://doi.org/10.1016/j.carbpol.2014.10.045.

Ghorbani, M., Roshangar, L., & Soleimani Rad, J. (2020). Development of reinforced chitosan/pectin scaffold by using the cellulose nanocrystals as nanofillers: An injectable hydrogel for tissue engineering. *European Polymer Journal, 130*, Article 109697. https://doi.org/10.1016/j.eurpolymj.2020.109697.

Hasan, N., Rahman, L., Kim, S. H., Cao, J., Arjuna, A., Lallo, S., et al. (2020). Recent advances of nanocellulose in drug delivery systems. In *Journal of pharmaceutical investigation, 50* pp. 553–572). Springer. https://doi.org/10.1007/s40005-020-00499-4.

Heise, K., Kontturi, E., Allahverdiyeva, Y., Tammelin, T., Linder, M. B., Nonappa, et al. (2021). Nanocellulose: Recent fundamental advances and emerging biological and biomimicking applications. *Advanced Materials, 33*(3), Article 2004349. https://doi.org/10.1002/adma.202004349.

Hoare, T. R., & Kohane, D. S. (2008). Hydrogels in drug delivery: Progress and challenges. In *Polymer, 49* pp. 1993–2007). Elsevier BV. https://doi.org/10.1016/j.polymer.2008.01.027.

Hua, S., Marks, E., Schneider, J. J., & Keely, S. (2015). Advances in oral nano-delivery systems for colon targeted drug delivery in inflammatory bowel disease: Selective targeting to diseased versus healthy tissue. In *Nanomedicine: Nanotechnology, biology, and medicine, 11* pp. 1117–1132). Elsevier Inc.. https://doi.org/10.1016/j.nano.2015.02.018.

Jordan, J. H., Easson, M. W., Dien, B., Thompson, S., & Condon, B. D. (2019). Extraction and characterization of nanocellulose crystals from cotton gin motes and cotton gin waste. *Cellulose, 26*(10), 5959–5979. https://doi.org/10.1007/s10570-019-02533-7.

Karasic, T. B., O'Hara, M. H., Loaiza-Bonilla, A., Reiss, K. A., Teitelbaum, U. R., Borazanci, E., et al. (2019). Effect of Gemcitabine and nab-Paclitaxel with or without hydroxychloroquine on patients with advanced pancreatic cancer: A phase 2 randomized clinical trial. *JAMA Oncology, 5*(7), 993–998. https://doi.org/10.1001/jamaoncol.2019.0684.

Khotimchenko, M. (2020). Pectin polymers for colon-targeted antitumor drug delivery. In *International journal of biological macromolecules, 158* pp. 1110–1124). Elsevier B. V.. https://doi.org/10.1016/j.ijbiomac.2020.05.002.

Kodoth, A. K., Ghate, V. M., Lewis, S. A., Prakash, B., & Badalamoole, V. (2019). Pectin-based silver nanocomposite film for transdermal delivery of Donepezil. *International Journal of Biological Macromolecules, 134*, 269–279. https://doi.org/10.1016/j.ijbiomac.2019.04.191.

Korsmeyer, R. W., Gurny, R., Doelker, E., Buri, P., & Peppas, N. A. (1983). Mechanisms of solute release from porous hydrophilic polymers. *International Journal of Pharmaceutics, 15*(1), 25–35. https://doi.org/10.1016/0378-5173(83)90064-9.

Laurén, P., Paukkonen, H., Lipiäinen, T., Dong, Y., Oksanen, T., Räikkönen, H., et al. (2018). Pectin and mucin enhance the bioadhesion of drug loaded nanofibrillated cellulose films. *Pharmaceutical Research, 35*(7). https://doi.org/10.1007/s11095-018-2428-z.

Li, Jian, Wang, Y., Zhang, L., Xu, Z., Dai, H., & Wu, W. (2019). Nanocellulose/gelatin composite cryogels for controlled drug release. *ACS Sustainable Chemistry and Engineering, 7*(6), 6381–6389. https://doi.org/10.1021/acssuschemeng.9b00161.

Li, J., Cai, C., Li, J., Li, J., Li, J., Sun, T., et al. (2018). Chitosan-based nanomaterials for drug delivery. In *Molecules, 23*. MDPI AG. https://doi.org/10.3390/molecules23102661.

Li, Y., Pang, H., Guo, Z., Lin, L., Dong, Y., Li, G., et al. (2014). Interactions between drugs and polymers influencing hot melt extrusion. *Journal of Pharmacy and Pharmacology, 66*(2), 148–166. https://doi.org/10.1111/jphp.12183. J Pharm Pharmacol.

Liu, C. Y., Zhong, G. J., Huang, H. D., & Li, Z. M. (2014). Phase assembly-induced transition of three dimensional nanofibril- to sheet-networks in porous cellulose with tunable properties. *Cellulose, 21*(1), 383–394. https://doi.org/10.1007/s10570-013-0096-z.

Liu, J., Liu, X., Han, Y., Zhang, J., Liu, D., Ma, G., et al. (2018a). Nanovaccine incorporated with hydroxychloroquine enhances antigen cross-presentation and promotes antitumor immune responses. *ACS Applied Materials and Interfaces, 10*(37), 30983–30993. https://doi.org/10.1021/acsami.8b09348.

Liu, Y., Sui, Y., Liu, C., Liu, C., Wu, M., Li, B., et al. (2018b). A physically crosslinked polydopamine/nanocellulose hydrogel as potential versatile vehicles for drug delivery and wound healing. *Carbohydrate Polymers, 188*(January), 27–36. https://doi.org/10.1016/j.carbpol.2018.01.093.

Mäntele, W., & Deniz, E. (2017). UV–VIS absorption spectroscopy: Lambert-Beer reloaded. *Spectrochimica Acta Part A: Molecular and Biomolecular Spectroscopy, 173*, 965–968. https://doi.org/10.1016/j.saa.2016.09.037.

Mariño, M. A., Rezende, C. A., & Tasic, L. (2018). A multistep mild process for preparation of nanocellulose from orange bagasse. *Cellulose, 25*(10), 5739–5750. https://doi.org/10.1007/s10570-018-1977-y.

Meneguin, A. B., Stringhetti, B., Cury, F., Santos, Dos, A., M., Franco, Faza, et al. (2017). Resistant starch/pectin free-standing films reinforced with nanocellulose intended for colonic methotrexate release. *Carbohydrate Polymers, 157*, 1013–1023. https://doi.org/10.1016/j.carbpol.2016.10.062.

Meng, Y., Wang, S., Guo, Z., Cheng, M., Li, J., & Li, D. (2020). Design and preparation of quaternized pectin-Montmorillonite hybrid film for sustained drug release. *International Journal of Biological Macromolecules, 154*, 413–420. https://doi.org/10.1016/j.ijbiomac.2020.03.140.

Minzanova, S. T., Mironov, V. F., Arkhipova, D. M., Khabibullina, A. V., Mironova, L. G., Zakirova, Y. M., et al. (2018). Biological activity and pharmacological application of pectic polysaccharides: A review. In *Polymers, 10*. MDPI AG. https://doi.org/10.3390/polym10121407.

Mironov, M. A., Shulepov, I. D., Ponomarev, V. S., & Bakulev, V. A. (2013). Synthesis of polyampholyte microgels from colloidal salts of pectinic acid and their application as pH-responsive emulsifiers. *Colloid and Polymer Science, 291*(7), 1683–1691. https://doi.org/10.1007/s00396-013-2903-3.

Mishra, R. K., Datt, M., & Banthia, A. K. (2008). Synthesis and characterization of pectin/pvp hydrogel membranes for drug delivery system. *AAPS PharmSciTech, 9*(2), 395–403. https://doi.org/10.1208/s12249-008-9048-6.

Mohamed, J. M., Alqahtani, A., Ahmad, F., Krishnaraju, V., & Kalpana, K. (2021). Pectin co-functionalized dual layered solid lipid nanoparticle made by soluble curcumin for the targeted potential treatment of colorectal cancer. *Carbohydrate Polymers, 252*. https://doi.org/10.1016/j.carbpol.2020.117180.

Moon, R. J., Martini, A., Nairn, J., Simonsen, J., & Youngblood, J. (2011). Cellulose nanomaterials review: Structure, properties and nanocomposites. *Chemical Society Reviews, 40*, 3941–3994. https://doi.org/10.1039/C0CS00108B.

Moraes, A. N. F., Silva, L. A. D., de Oliveira, M. A., de Oliveira, E. M., Nascimento, T. L., Lima, E. M., et al. (2020). Compatibility study of hydroxychloroquine sulfate with pharmaceutical excipients using thermal and nonthermal techniques for the development of hard capsules. *Journal of Thermal Analysis and Calorimetry, 140*(5), 2283–2292. https://doi.org/10.1007/s10973-019-08953-8.

Moslemi, M. (2021). Reviewing the recent advances in application of pectin for technical and health promotion purposes: From laboratory to market. *Carbohydrate Polymers, 254*, Article 117324. https://doi.org/10.1016/j.carbpol.2020.117324.

Nascimento, J. U., Zambuzi, G. C., Ferreira, J. O., Paula, J. H., Ribeiro, T. S., Souza, A. L., et al. (2019). A simple process to tune wettability of pectin-modified silanized glass. *Colloids and Surfaces A: Physicochemical and Engineering Aspects, 577*, 67–74. https://doi.org/10.1016/j.colsurfa.2019.05.056.

Nascimento, S. A., & Rezende, C. A. (2018). Combined approaches to obtain cellulose nanocrystals, nanofibrils and fermentable sugars from elephant grass. *Carbohydrate Polymers, 180*(August 2017), 38–45. https://doi.org/10.1016/j.carbpol.2017.09.099.

Nasrollahzadeh, M., Sajjadi, M., Iravani, S., & Varma, R. S. (2021). Starch, cellulose, pectin, gum, alginate, chitin and chitosan derived (nano)materials for sustainable water treatment: A review. In *Carbohydrate polymers, 251*. Elsevier Ltd. https://doi.org/10.1016/j.carbpol.2020.116986.

Nawrocka, A., Szymańska-Chargot, M., Miś, A., Wilczewska, A. Z., & Markiewicz, K. H. (2017). Effect of dietary fibre polysaccharides on structure and thermal properties of gluten proteins – A study on gluten dough with application of FT-Raman spectroscopy, TGA and DSC. *Food Hydrocolloids, 69*, 410–421. https://doi.org/10.1016/j.foodhyd.2017.03.012.

Niu, W., Chen, X., Xu, R., Dong, H., Yang, F., Wang, Y., et al. (2021). Polysaccharides from natural resources exhibit great potential in the treatment of ulcerative colitis: A review. In *Carbohydrate polymers, 254*. Elsevier Ltd, Article 117189. https://doi.org/10.1016/j.carbpol.2020.117189.

Noronha, V. T., Camargos, C. H. M., Jackson, J. C., Souza Filho, A. G., Paula, A. J., Rezende, C. A., et al. (2021). Physical membrane-stress-mediated antimicrobial properties of cellulose nanocrystals. *ACS Sustainable Chemistry and Engineering, 9*, 3203–3212. https://doi.org/10.1021/acssuschemeng.0c08317.

Oliveira, A. C., de, J., Chaves, L. L., Ribeiro, F., de, O. S., de Lima, L. R. M., et al. (2021). Microwave-initiated rapid synthesis of phthalated cashew gum for drug delivery systems. *Carbohydrate Polymers, 254*, Article 117226. https://doi.org/10.1016/j.carbpol.2020.117226.

Pastore, M. N., Kalia, Y. N., Horstmann, M., & Roberts, M. S. (2015). Transdermal patches: History, development and pharmacology. In *British journal of pharmacology, 172* pp. 2179–2209). John Wiley and Sons Inc.. https://doi.org/10.1111/bph.13059.

Paulraj, T., Riazanova, A. V., & Svagan, A. J. (2018). Bioinspired capsules based on nanocellulose, xyloglucan and pectin – The influence of capsule wall composition on permeability properties. *Acta Biomaterialia, 69*, 196–205. https://doi.org/10.1016/j.actbio.2018.01.003.

Peppas, N. A., & Khare, A. R. (1993). Preparation, structure and diffusional behavior of hydrogels in controlled release. In *Advanced drug delivery reviews, 11*.

Perche, F., Yi, Y., Hespel, L., Mi, P., Dirisala, A., Cabral, H., et al. (2016). Hydroxychloroquine-conjugated gold nanoparticles for improved siRNA activity. *Biomaterials, 90*, 62–71. https://doi.org/10.1016/j.biomaterials.2016.02.027.

Pereira, P. H. F., Ornaghi Júnior, H. L., Coutinho, L. V., Duchemin, B., & Cioffi, M. O. H. (2020). Obtaining cellulose nanocrystals from pineapple crown fibers by free-chlorite hydrolysis with sulfuric acid: Physical, chemical and structural characterization. *Cellulose, 27*(10), 5745–5756. https://doi.org/10.1007/s10570-020-03179-6.

Ponrasu, T., Chen, B. H., Chou, T. H., Wu, J. J., & Cheng, Y. S. (2021). Fast dissolving electrospun nanofibers fabricated from jelly fig polysaccharide/pullulan for drug delivery applications. *Polymers, 13*(2), 1–17. https://doi.org/10.3390/polym13020241.

Raghav, N., Sharma, M. R., & Kennedy, J. F. (2021). Nanocellulose: A mini-review on types and use in drug delivery systems. *Carbohydrate Polymer Technologies and Applications, 2*, Article 100031. https://doi.org/10.1016/J.CARPTA.2020.100031.

Richard, S. A., Kampo, S., Hechavarria, M. E., Sackey, M., Buunaaim, A. D. B., Kuugbee, E. D., et al. (2020). Elucidating the pivotal immunomodulatory and anti-inflammatory potentials of chloroquine and hydroxychloroquine. *Journal of Immunology Research, 2020*, 1–13. https://doi.org/10.1155/2020/4582612.

Sadr, M. S., Heydarinasab, A., Panahi, H. A., & Javan, R. S. (2021). Production and characterization of biocompatible nano-carrier based on Fe_3O_4 for magnetically hydroxychloroquine drug delivery. *Polymers for Advanced Technologies, 32*(2), 564–573. https://doi.org/10.1002/pat.5110.

Saini, B., & Bansal, G. (2013). Characterization of four new photodegradation products of hydroxychloroquine through LC-PDA, ESI-MSn and LC-MS-TOF studies. *Journal of Pharmaceutical and Biomedical Analysis, 84*, 224–231. https://doi.org/10.1016/j.jpba.2013.06.014.

Saito, T., Kimura, S., Nishiyama, Y., & Isogai, A. (2007). Cellulose nanofibers prepared by TEMPO-mediated oxidation of native cellulose. *Biomacromolecules, 8*(8), 2485–2491. https://doi.org/10.1021/bm0703970.

Sheikhi, A., Hayashi, J., Eichenbaum, J., Gutin, M., Kuntjoro, N., Khorsandi, D., et al. (2019). Recent advances in nanoengineering cellulose for cargo delivery. *Journal of Controlled Release : Official Journal of the Controlled Release Society, 294*, 53. https://doi.org/10.1016/J.JCONREL.2018.11.024.

Silva, L. E., dos Santos, A., de, A., Torres, L., McCaffrey, Z., Klamczynski, A., et al. (2021). Redispersion and structural change evaluation of dried microfibrillated cellulose. *Carbohydrate Polymers, 252*, Article 117165. https://doi.org/10.1016/j.carbpol.2020.117165.

Silva Favacho, H. A., do Couto, R. O., Duarte, M. P. F., Peixoto, M. P. G., Lopez, R. F. V., Pedrazzi, V., … Freitas, O. (2020). Synergy between surfactants and mucoadhesive polymers enhances the transbuccal permeation of local anesthetics from freeze-dried tablets. *Materials Science and Engineering C, 108*. https://doi.org/10.1016/j.msec.2019.110373.

Siqueira, G., Bras, J., & Dufresne, A. (2010). Cellulosic bionanocomposites: A review of preparation, properties and applications. *Polymers, 2*, 728–765. https://doi.org/10.3390/polym2040728.

Slavutsky, A. M., & Bertuzzi, M. A. (2019). Formulation and characterization of hydrogel based on pectin and brea gum. *International Journal of Biological Macromolecules, 123*, 784–791. https://doi.org/10.1016/j.ijbiomac.2018.11.038.

Sleightholm, R., Yang, B., Yu, F., Xie, Y., & Oupický, D. (2017). Chloroquine-modified hydroxyethyl starch as a polymeric drug for cancer therapy. *Biomacromolecules, 18*(8), 2247–2257. https://doi.org/10.1021/acs.biomac.7b00023.

Sosnik, A. (2014). Alginate particles as platform for drug delivery by the oral route: State-of-the-art. *ISRN Pharmaceutics, 2014*, 1–17. https://doi.org/10.1155/2014/926157.

Sriamornsak, P. (2003). Chemistry of pectin and its pharmaceutical uses: A review. *Silpakorn University International Journal, 3*, 206–228. https://www.scienceopen.com/document?vid=4b41efab-8222-4f0d-9ade-2559a820718c.

Anirudhan, T. S., Chithra, S. V, Shainy, F., & Thomas, J. P. (2019). Effect of dual stimuli responsive dextran/nanocellulose polyelectrolyte complexes for chemophotothermal synergistic cancer therapy. *International Journal of Biological Macromolecules, 135*, 776–789. https://doi.org/10.1016/j.ijbiomac.2019.05.218.

Thomas, S. K., Begum, P. M. S., Midhun Dominic, C. D., Salim, N. V., Hameed, N., Rangappa, S. M., et al. (2021). Isolation and characterization of cellulose nanowhiskers from *Acacia caesia* plant. *Journal of Applied Polymer Science, 138*(15), 50213. https://doi.org/10.1002/app.50213.

United States pharmacopeia 34th ed Rockville (MD): US Pharmacop | Gaba Signaling. (n. d.). Retrieved March 11, 2021, from https://gabasignaling.com/united-states-pharmacopeia-34th-ed-rockville-md-us-pharmacop/.

Vityazev, F. V., Fedyuneva, M. I., Golovchenko, V. V., Patova, O. A., Ipatova, E. U., Durnev, E. A., et al. (2017). Pectin-silica gels as matrices for controlled drug release in gastrointestinal tract. *Carbohydrate Polymers, 157*, 9–20. https://doi.org/10.1016/j.carbpol.2016.09.048.

Wang, S., Meng, Y., Li, J., Liu, J., Liu, Z., & Li, D. (2020). A novel and simple oral colon-specific drug delivery system based on the pectin/modified nano-carbon sphere nanocomposite gel films. *International Journal of Biological Macromolecules, 157*, 170–176. https://doi.org/10.1016/j.ijbiomac.2020.04.197.

Wang, T., Hu, Q., Zhou, M., Xia, Y., Nieh, M. P., & Luo, Y. (2016a). Development of "all natural" layer-by-layer redispersible solid lipid nanoparticles by nano spray drying technology. *European Journal of Pharmaceutics and Biopharmaceutics, 107*, 273–285. https://doi.org/10.1016/j.ejpb.2016.07.022.

Wang, Yang, Shi, K., Zhang, L., Hu, G., Wan, J., Tang, J., et al. (2016b). Significantly enhanced tumor cellular and lysosomal hydroxychloroquine delivery by smart liposomes for optimal autophagy inhibition and improved antitumor efficiency with liposomal doxorubicin. *Autophagy, 12*(6), 949–962. https://doi.org/10.1080/15548627.2016.1162930.

Wang, Ying, Zhou, Z., Chen, W., Qin, M., Zhang, Z., Gong, T., et al. (2018). Potentiating bacterial cancer therapy using hydroxychloroquine liposomes. *Journal of Controlled Release, 280*, 39–50. https://doi.org/10.1016/j.jconrel.2018.04.046.

Wei, X., Senanayake, T. H., Warren, G., & Vinogradov, S. V. (2013). Hyaluronic acid-based nanogel-drug conjugates with enhanced anticancer activity designed for the targeting of cd44-positive and drug-resistant tumors. *Bioconjugate Chemistry, 24*(4), 658–668. https://doi.org/10.1021/bc300632w.

Wong, T. W., Colombo, G., & Sonvico, F. (2011). Pectin matrix as oral drug delivery vehicle for colon cancer treatment. In *AAPS pharmscitech, 12* pp. 201–214). AAPS PharmSciTech. https://doi.org/10.1208/s12249-010-9564-z.

Yan, F., Cao, H., Cover, T. L., Washington, M. K., Shi, Y., Liu, L. S., et al. (2011). Colon-specific delivery of a probiotic-derived soluble protein ameliorates intestinal inflammation in mice through an EGFR-dependent mechanism. *Journal of Clinical Investigation, 121*(6), 2242–2253. https://doi.org/10.1172/JCI44031.

Yin, S., Xia, C., Wang, Y., Wan, D., Rao, J., Tang, X., et al. (2018). Dual receptor recognizing liposomes containing paclitaxel and hydroxychloroquine for primary and metastatic melanoma treatment via autophagy-dependent and independent pathways. *Journal of Controlled Release, 288*, 148–160. https://doi.org/10.1016/j.jconrel.2018.08.015.

Zhang, W., Fan, X., Gu, X., Gong, S., Wu, J., Wang, Z., et al. (2020). Emulsifying properties of pectic polysaccharides obtained by sequential extraction from black tomato pomace. *Food Hydrocolloids, 100*. https://doi.org/10.1016/j.foodhyd.2019.105454.